

Structure, Stability, Thermodynamic Properties, and IR Spectra of the Protonated Water Decamer $\text{H}^+(\text{H}_2\text{O})_{10}$

S. Karthikeyan and Kwang S. Kim*

Center for Superfunctional Materials, Department of Chemistry, Pohang University of Science and Technology, San 31, Hyojadong, Namgu, Pohang 790-784, Korea

Received: May 6, 2009; Revised Manuscript Received: June 20, 2009

Protonated water clusters $\text{H}^+(\text{H}_2\text{O})_n$ favor two-dimensional (2D) structures for $n \leq 7$ at low temperatures. At 0 K, the 2D and three-dimensional (3D) structures for $n = 8$ are almost isoenergetic, and the 3D structures for $n > 9$ tend to be more stable. However, for $n = 9$, the netlike structures are likely to be more stable above 150 K. In this regard, we investigate the case of $n = 10$ to find which structure is more stable between the 3D structure and the netlike structure around 150 and 250 K. We use density functional theory, Møller–Plesset second-order perturbation theory, and coupled cluster theory with single, double, and perturbative triple excitations (CCSD(T)). At the complete basis set limit for the CCSD(T) level of theory, three isomers of 3D cage structure are much more stable in zero point energy corrected binding energy and in free binding energies at 150 K than the lowest energy netlike structures, while the netlike structure would be more stable around ~ 250 K. The predicted vibrational spectra are in good agreement with the experiment. One of the three isomers explains the experimental IR observation of an acceptor (A) type peak of a dangling hydrogen atom.

Introduction

The protonated water clusters $\text{H}^+(\text{H}_2\text{O})_n$ have been extensively studied^{1–3} because of their importance in the atmosphere, biosphere, and acid–base chemistry in solution. Nevertheless, high levels of ab initio calculations have been limited to only small clusters ($n \leq 9$). As n increases, the number of possible configurations increases exponentially, and it is difficult to find the global minimum energy structures at a given finite temperature.

There has been a controversial issue over the two-dimensional (2D) versus three-dimensional (3D) structure for $n = 7–9$ of the protonated water clusters. For $n \leq 6$, 2D structures are found to be more stable in most calculations.⁴ For $n = 7$, the 3D structure is predicted to be lower in energy than the 2D structure at most levels of theory without ZPE correction. However, at the coupled cluster theory with single, double, and perturbative triple excitations (CCSD(T))/complete basis set (CBS) limit, the 2D Zundel-type structure is the most stable, though it is nearly isoenergetic to the 3D structure.⁵ For $n = 8$, at 0 K the 2D and 3D structures are almost isoenergetic.⁶ The 3D structures tend to be more stable for $n \geq 9$. However, above 150 K at which most experiments were done, the netlike structures tend to be more stable for $n = 9$.⁷ On the other hand, it is well-known that for $n = 21$, the dodecahedral structure is the most stable at ~ 200 K.⁸ Therefore, there should be the transition at ~ 150 K from netlike structure to closed 3D structure for clusters larger than a critical size. In this regard, we investigate the case of $n = 10$ to find out whether the netlike structure would still be more stable around 150 K than the closed 3D structure.

For $\text{H}^+(\text{H}_2\text{O})_{n=10}$, Miyazaki et al.² proposed a netlike structure based on the experimental data around 200–250 K. According to Headrick et al.,¹ around ~ 150 K two strong peaks around 3700 cm^{-1} appear and persist throughout $n = 20$, while two very weak peaks reflecting a small population of the free OH (which disappears from $n = 11$) still remain. This indicates that

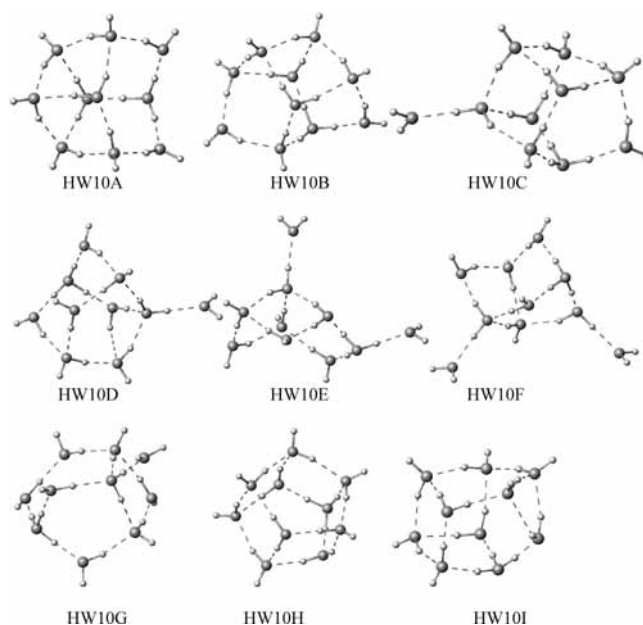


Figure 1. Low-energy structures of the $\text{H}^+(\text{H}_2\text{O})_{10}$ cluster.

the structure around 200–250 K would have netlike water molecules, while the structure around 150 K would have a closed form with no extra water molecule or no more than one extra water molecule. Thus, we need to carry out high level ab initio calculations to correctly understand the structure for $n = 10$.

In the protonated water clusters, two primary charge carriers of Eigen form⁹ and a Zundel form¹⁰ play an important role. This has raised the question of which form would be more stable for the given n . The structural change of the protonated water clusters with increasing cluster size has been carried out.^{1–8,11} We note that protonated water clusters are quite different in structure from neutral water clusters,^{12,13} anionic water clusters,^{14,15} and water clusters containing a cation.¹⁶ Similarly, the experi-

* Corresponding author, kim@postech.ac.kr.

TABLE 1: B3LYP/aVDZ Interaction Energies (ΔE_c , ΔE_0) and Thermodynamic Quantities (Enthalpy, ΔH_{150K} ; Free Energy, ΔG_{150K}) As Well As Their Relative Values (δE_c , δE_0 , δH_{150K} , δG_{150K}) in kcal/mol for Low-Energy Structures of $H^+(H_2O)_{10}$ ^a

structure	δE_c	δE_0	δH_{150K}	δG_{150K}
HW10A	0.00	0.00	0.00	1.23
HW10B	0.23	0.04	0.05	1.24
HW10C	0.44	0.36	0.16	0.68
HW10D	2.53	0.42	1.14	0.38
HW10E	4.54	0.78	1.92	0.00
HW10F	3.58	0.89	1.89	0.39
HW10G	3.33	0.92	1.79	0.49
HW10H	2.25	2.74	2.52	4.37
HW10I	2.95	3.25	3.15	4.69
	$-\Delta E_c$	$-\Delta E_0$	$-\Delta H_{150K}$	$-\Delta G_{150K}$
HW10A	155.60	131.83	138.87	95.68

^a The most stable structures at 0 and 150 K are given in boldface type.

mental vibrational spectra^{1,2} for $H^+(H_2O)_{10}$ do not corroborate the bipental structure of the neutral water decamer.¹⁷ Thus, to find the correct structure of $H^+(H_2O)_{10}$, we have carried out density functional theory (DFT), Møller–Plesset second-order perturbation theory (MP2), and CCSD(T) calculations. To obtain the right conclusion, we have focused our attention to the following: (a) binding energy at high levels of theory, (b) zero

point energy (ZPE) correction, (c) complete basis set limit values, and (d) comparison of the DFT and MP2 predicted spectra with the available experimental spectra.¹

Computational Method

To find the global minimum energy structure, we employed the basin-hopping global optimization¹⁸ with the density functional based tight-binding (DFTB) method.¹⁹ In addition, we considered the previously reported low energy geometries.¹¹ For the low-lying energy structures explored by basin-hopping global optimization, we carried out geometry optimization and total energy calculations using Becke’s three parameters with the Lee–Yang–Parr (B3LYP)²⁰ functional, MP2, and CCSD(T). All atoms were treated with the aug-cc-pVDZ and aug-cc-pVTZ basis sets (which will be abbreviated as aVDZ, and aVTZ, respectively). The harmonic vibrational frequencies, ZPEs, and thermodynamic quantities were evaluated on the B3LYP/aVDZ and MP2/aVDZ optimized geometries. We also carried out CCSD(T)/aVDZ single point energy calculations using the MP2/aVDZ optimized geometries. The basis set superposition error (BSSE) correction was made after geometry optimization. The B3LYP and MP2 calculations were performed with the Gaussian 03 suite of programs,²¹ and the CCSD(T) calculations were done with the MOLPRO suite.²² The molecular structures were drawn with the POSMOL package.²³

We estimated the MP2/CBS binding energies using the extrapolation scheme, which utilizes that the electron correlation

TABLE 2: The MP2 and CCSD(T) Interaction Energies (ΔE_c , ΔE_0) and Thermodynamic Quantities (Enthalpy, ΔH_{150K} ; Free Energy, ΔG_{150K} , ΔG_{250K}) As Well As Their Relative Values (δE_c , δE_0 , δH_{150K} , δG_{150K} , δG_{250K}) in kcal/mol for Low-Energy Structures of $H^+(H_2O)_{10}$ ^a

MP2	aVDZ		aVTZ		CBS			CCSD(T)/aVDZ	
	δE_c	δE_0	δE_c	δE_0	δE_c	δE_0	δG_{150K}	δE_c	δE_0
HW10A	0.00	0.00	0.00	0.00	0.00	0.00	0.00	0.00	0.00
HW10B	0.38	0.28	0.22	0.12	0.16	0.06	0.30	0.29	0.19
HW10C	0.43	0.48	0.56	0.60	0.61	0.66	0.49	0.33	0.37
HW10D	3.84	2.15	3.94	2.25	3.98	2.29	4.40	3.97	2.28
HW10E	5.20	1.76	5.43	1.99	5.52	2.09	3.51	5.42	1.99
HW10F	3.77	1.27	4.14	1.64	4.30	1.80	3.50	3.92	1.42
HW10G	4.24	1.87	4.30	1.94	4.33	1.96	3.35	4.46	2.10
HW10H	1.99	2.49	1.88	2.38	1.84	2.34	6.16	1.89	2.39
HW10I	2.29	2.42	2.35	2.49	2.38	2.51	6.11	2.12	2.26
	$-\Delta E_c$	$-\Delta E_0$	$-\Delta E_c$	$-\Delta E_0$	$-\Delta E_c$	$-\Delta E_0$	$-\Delta G_{150K}$	$-\Delta E_c$	$-\Delta E_0$
HW10A	146.43	122.42	153.60	129.60	156.63	132.62	99.95	144.75	120.75
CCSD(T)	CBS		CBS ^M			CBS ^D			
	δE_c	δE_0	δH_{150K}	δG_{150K}	δG_{250K}	δE_0	δH_{150K}	δG_{150K}	δG_{250K}
HW10A	0.00	0.04	0.00	0.00	0.00	0.00	0.00	0.67	2.63
HW10B	0.06	0.00	0.10	0.20	0.15	0.09	0.11	0.73	2.67
HW10C	0.51	0.59	0.21	0.39	0.66	0.24	0.04	0.00	1.45
HW10D	4.11	2.46	4.35	4.53	4.28	1.85	2.58	1.26	1.77
HW10E	5.75	2.35	4.62	3.74	4.79	1.67	2.81	0.33	0.00
HW10F	4.45	1.98	4.15	3.65	4.29	1.23	2.23	0.17	0.13
HW10G	4.56	2.23	4.37	3.57	4.45	2.06	2.92	1.06	1.20
HW10H	1.74	2.28	3.29	6.06	2.71	2.38	2.16	3.45	5.88
HW10I	2.21	2.39	3.55	5.95	3.10	2.43	2.32	3.30	5.50
	$-\Delta E_c$	$-\Delta E_0$	$-\Delta H_{150K}$	$-\Delta G_{150K}$	$-\Delta G_{250K}$	$-\Delta E_0$	$-\Delta H_{150K}$	$-\Delta G_{150K}$	$-\Delta G_{250K}$
HW10A	154.95	130.95	139.23	98.28	140.02	120.98	128.02	84.83	55.59

^a The BSSE corrections were made. CCSD(T)/CBS energies were estimated by applying the correction term (the difference between MP2/aVDZ and CCSD(T)/aVDZ energies) to the MP2/CBS interaction energies which were obtained with the extrapolation scheme utilizing the electron correlation proportional to N^3 for the aug-cc-pVNZ basis set. CBS^M values are calculated based on MP2 frequencies, while CBS^D values are calculated based on B3LYP frequencies. The most stable structures at 0 and 150 K (250 K) for the MP2/CBS and CCSD(T)/CBS levels are given in boldface type.

TABLE 3: Vibrational Frequencies (cm^{-1}) of $\text{H}^+(\text{H}_2\text{O})_{10}$ Predicted by B3LYP/aVDZ (Scale Factor, 0.976) and MP2/aVDZ (Scale Factor, 0.956), and the Experimental Frequencies (Reference 1)^a

mode	B3LYP/aVDZ					MP2/aVDZ					expt. ¹
	HW10A	HW10B	HW10C	HW10E	HW10F	HW10A	HW10B	HW10C	HW10E	HW10F	
$\nu_a \text{AH}_d$			3741w	3742w	3739w			3749w	3748w, 3743w	3747w, 3745w	3738w
νADH_d	3708w, 3704w	3715w, 3705w	3707w	3714w, 3712w,	3715w, 3708w,	3703w, 3699w	3712w, 3702w	3702w	3717w, 3712w,	3717w, 3703w,	3716m
$\nu_s \text{AADH}_d$	3690w, 3684w, 3682w, 3679w	3688w, 3686w, 3685w, 3675w	3690w, 3687w, 3682w, 3681w	3691w, 3680w 3683w	3687w, 3683w, 3679w, 3674w	3687w, 3683w, 3679w, 3674w	3684w, 3683w, 3678w, 3669w	3686w, 3684w, 3677w, 3675w	3687w, 3687w, 3677w, 3675w	3686w, 3687w, 3677w, 3677w	3689s
$\nu_s \text{AH}_d$			3643w	3643w	3641w			3630w	3629w, 3625w	3629w, 3627w	3650w
$\nu_a \text{ADDH}_h$	3625m, 3535m	3596s, 3520m	3610s, 3519m	3529m	3531m	3590m, 3495w	3563s, 3480m	3572m, 3477m	3491m, 3416s	3485m, 3405m	3600m
$\nu_a \text{AADDH}_h$			3576m	3440m	3439m			3533m	3416s	3405m	
$\nu_s \text{ADDH}_h$	3561w, 3483w	3532m, 3432m	3547w, 3439w	3497m	3554m	3504m, 3429w	3478m, 3390m	3488m, 3406w	3461m, 3406w	3511w, 3406w	3520w
νAADH_h	3436s, 3421w, 3350s, 3327m, 3097m	3442m, 3370m, 3318w, 3199s, 3027m	3433m, 3349m, 3283s, 3056s	3428m, 3227w, 3192m	3428m, 3196s	3404m, 3391w, 3331m, 3309m, 3119m	3344m, 3299m, 3199s, 3054s	3406m, 3325m, 3265m, 3057m	3386w, 3251s, 3210w, 3194m	3391m, 3338m, 3172s	3430s
νADH_h	3407w, 3387m	3523w, 3403m	3391w	3392m, 3331w	3396m, 3367s	3377w, 3364w	3489m, 3406m, 3367w	3365w	3355m	3362m, 3236s	3350s
$\nu_s \text{AADDH}_h$			3374s	3266s,	3358m			3337m	3292m	3330m	
$\nu_s \text{H}_3\text{O}^+$	2858m	2911m	2927m	3221m	2896m	2832m	2900s	2910s	3167s	2865s	2820w
$\nu_a \text{H}_3\text{O}^+$	2717s, 2477s	2733m, 2278s	2725s, 2269s	2944s	2734s, 2295s	2736s, 2463s	2745s, 2306s	2737s, 2263s	2908s	2731s, 2297s	2730w
$\nu \text{H}_3\text{O}^+$ bend	1729w, 1661w	1716w, 1670w	1729w, 1660w	1722w, 1696w	1674w, 1658w	1723w, 1651w	1709w, 1663w	1720w, 1651w	1719s, 1686w	1671w	1620w

^a Key: ν , stretching mode; ν_s/ν_a , symmetric/asymmetric stretching modes; H_d , dangling hydrogen seen in A, AD, and AAD types of the hydrogen bonding of H_2O ; H_h , hydrogen bonded hydrogen. IR intensities are denoted in subscripts (s, strong; m, medium; w, weak). The predicted peaks are marked in boldface type when their intensity is in reasonable agreement with the experimental intensity.

is proportional to N^{-3} for the aug-cc-pVNZ basis sets.^{24,25} The CCSD(T)/CBS energies were estimated by assuming that the difference in binding energies between MP2/aVDZ and MP2/CBS calculations is similar to that between CCSD(T)/aVDZ and CCSD(T)/CBS calculations.^{25,26} The ZPE and thermal energies at the MP2/aVDZ level were used to evaluate those of the MP2 and CCSD(T) calculations using other basis sets.

The spectral features of $\text{H}^+(\text{H}_2\text{O})_{10}$ were investigated at the B3LYP/aVDZ and MP2/aVDZ levels of theory whose frequencies were scaled by 0.976 and 0.956, respectively, to match the average value of $-\text{OH}$ stretching frequencies of the water monomer with the experimental value.²⁷

Results and Discussion

The important low-energy structures of $\text{H}^+(\text{H}_2\text{O})_{10}$ are shown in Figure 1. The binding energies and thermodynamic properties were calculated at the B3LYP/aVDZ level and at the CBS limit of the MP2 and CCSD(T) levels of theory. In the protonated water cluster, each hydrogen atom of the H_3O^+ ion involves a hydrogen bond as a strong hydrophilic site, whereas the oxygen atom of the H_3O^+ ion behaves as a hydrophobic site due to the three positively charged hydrogen atoms that hinder the close approach toward the oxygen center from other hydrogen atoms.⁵ The H_3O^+ ion tends to be on the surface of the cluster, where the three hydrogen atoms of the H_3O^+ ion are bonded by three water molecules. Thus, the H_3O^+ ion favors the trihydrogen bonded structure.

The hydrogen bond arrangement has a significant effect on the structure as well as energy of the cluster. In Figure 1, HW10A, HW10B, HW10H, and HW10I are completely closed 3D structures, while HW10C, HW10D, and HW10G are 3D structures with one dangling water molecule outside the cage structure, and HW10E and HW10F are netlike structures. Then, the completely closed 3D structures would be the most stable at 0 K unless there is too much strain by compact packing in HW10H or by a strained three-membered ring in HW10I. The entropy effect would favor eventually the netlike structures as the temperature increases. Thus, it would be important to know the structural changes of the cluster depending on the temperature.

The predicted binding energies and thermodynamic quantities of isomers of $\text{H}^+(\text{H}_2\text{O})_{10}$ at the B3LYP/aVDZ level are listed in Table 1. Among the isomers, HW10A is the lowest energy structure in ZPE-uncorrected energy (ΔE_c), while HW10A, HW10B, and HW10C are nearly isoenergetic in ZPE-corrected energy (ΔE_0). However, HW10E is more stable than other isomers in free energy (ΔG) at 150 K. Thus, we have further investigated them at higher levels of theory. The energies and thermodynamic quantities of the isomers at the MP2/aVDZ, MP2/aVTZ, MP2/CBS, CCSD(T)/aVDZ, and CCSD(T)/CBS levels are given in Table 2. Since the thermal energies were calculated only at the B3LYP/aVDZ and MP2/aVDZ levels, the CCSD(T)/CBS values were evaluated with both B3LYP/aVDZ and MP2/aVDZ values; the CBS^M values were calculated

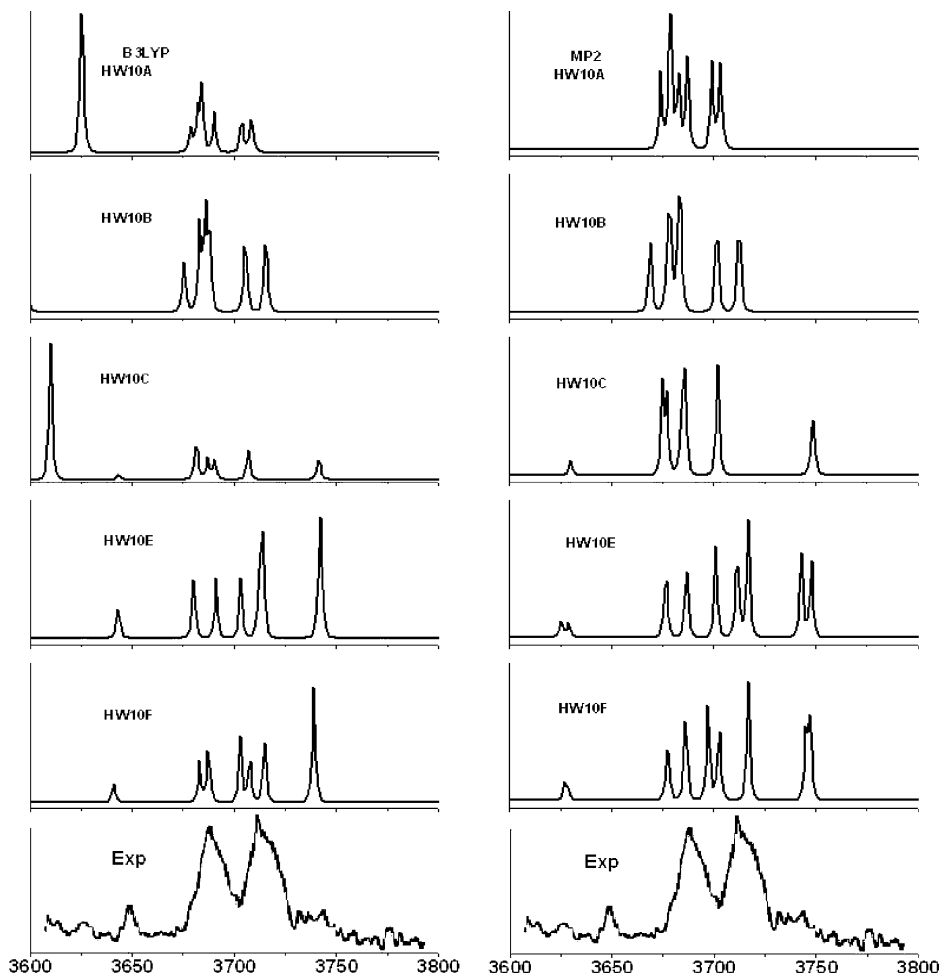


Figure 2. B3LYP/aVDZ (scale factor, 0.976) and MP2/aVDZ (scale factor, 0.956) predicted vibrational spectra of the HW10A, HW10B, HW10C, HW10E, and HW10F structures for the $\text{H}^+(\text{H}_2\text{O})_{10}$ cluster, which are compared with the experimental spectra in the 3600–3800 cm^{-1} region (ref 1).

using the MP2/aVDZ thermal energies, while the CBS^D values were calculated using the B3LYP/aVDZ thermal energies.

The isomers HW10A, HW10B, and HW10C are isoenergetic; these isomers are more stable than other isomers, because these have more hydrogen bonds than other structures except highly strained structures of HW10H and HW10I. The zero-point vibrations show significant effects on altering the relative stability of these isomers. The effects are particularly noticeable between open (HW10E, HW10F, and HW10G) and closed isomers.

At the MP2/CBS and CCSD(T)/CBS^M levels, two lowest energy structures HW10A and HW10B are nearly isoenergetic in ΔE_e , ΔE_0 , $\Delta G_{150\text{K}}$, and $\Delta G_{250\text{K}}$. The next lowest energy structure is HW10C, which is slightly higher by only a fraction of kcal/mol. These three isomers are more stable than other isomers by ~ 4 kcal/mol in free energy. This leads us to conjecture if the three structures of HW10A, HW10B, and HW10C could have been the most populated in the experiments carried out around ~ 150 and ~ 250 K. However, at the CCSD(T)/CBS^D levels, the most stable structures at ~ 150 K are HW10C and HW10F, and those at ~ 250 K are HW10E and HW10F, because the thermal energies calculated by B3LYP/aVDZ and MP2/aVDZ are somewhat different. Here, we note that the CCSD(T)/CBS^D results better explain the experiments carried out around ~ 150 – 175 K and ~ 200 – 250 K. In this regard, CCSD(T)/CBS^D results would be more reliable. This is partly due to the fact that the MP2 frequencies were calculated

without BSSE correction because the BSSE-corrected frequency calculations based on the numerical approach are not feasible for this large size of clusters. The BSSE-uncorrected MP2 frequencies tend to somewhat overestimate the ZPEs because the H-bonding energies are overestimated.²⁸ Thus, the thermal energy corrections with the B3LYP results would be more reliable in the present system.

In water clusters and protonated water clusters, the spectral shifts are found to be strongly dependent on the number of donors, whereas their dependency on the number of acceptors is rather small.^{16,29} Each type of molecule in the hydrogen bonded clusters tends to show its own characteristic frequency shifts depending on its H-bond type. Many previous vibrational frequencies reported by experiments are mostly based on the OH stretching modes of the water molecule, while few experiments reported the motion of the proton involving with the interconversion between the Eigen and Zundel type ion clusters.^{1–3} The vibrations associated with the excess proton in these clusters occur at much lower frequencies than the general OH stretching frequencies. Thus, we also considered the spectral region below the OH vibrational stretching frequencies.

The experimental IR spectrum of $\text{H}^+(\text{H}_2\text{O})_{10}$ indicates the acceptor (A) type asymmetric and symmetric OH stretching peaks.¹ It shows dangling hydrogen atoms of tricoordinated H_2O (acceptor–acceptor–donor (AAD) type), bicoordinated H_2O (acceptor–donor (AD) type), and symmetric and asymmetric uncoordinated H_2O (acceptor (A)). The B3LYP/aVDZ and

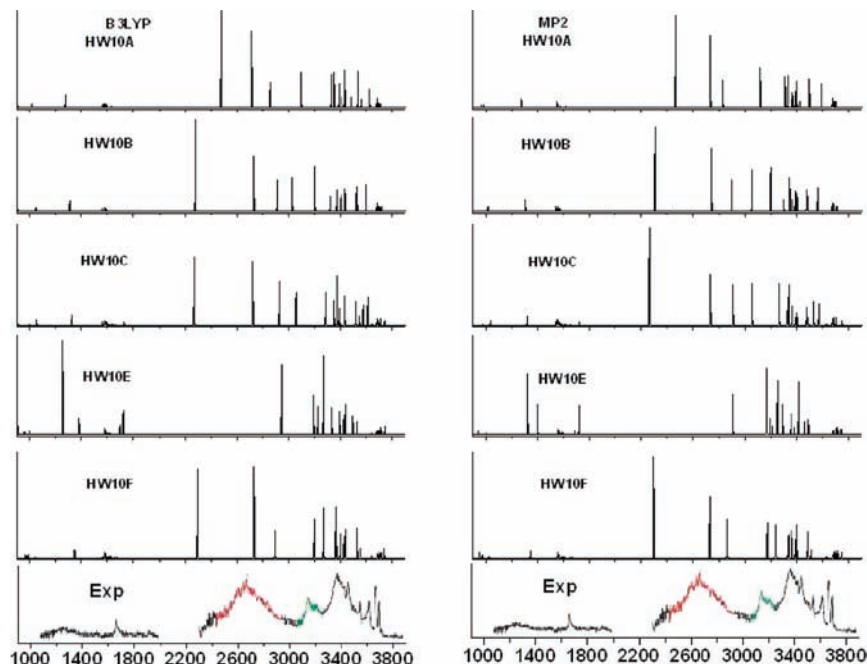


Figure 3. Same as Figure 2 in the 900–3800 cm^{-1} region.

MP2/aVDZ frequencies are compared with the available experimental vibrational frequencies¹ in Table 3, Figure 2 (3600–3800 cm^{-1}), and Figure 3 (900–3800 cm^{-1}). The combined vibrational frequencies of HW10C and HW10F isomers are in good agreement with the experimentally reported vibrational frequencies. Although both B3LYP/aVDZ and MP2/aVDZ vibrational frequencies are similar, the B3LYP/aVDZ thermal energies would be more reliable, as discussed earlier. Thus, our discussion will be given based on the B3LYP/aVDZ frequencies.

A single proton acceptor (A-water) with a dangling hydrogen atom (H_d) terminates the hydrogen bond net. In this case, the asymmetric ($\nu_a\text{AH}_d$) and symmetric ($\nu_s\text{AH}_d$) stretching vibrations of free OH bonds in structures of HW10C, HW10E, and HW10F appear at ~ 3740 and ~ 3642 cm^{-1} , respectively, consistent with the experimental frequencies at 3738 and 3650 cm^{-1} . A hydrogen bond net contains dicoordinated water molecules of single acceptor–single donor (AD-water). The calculated frequencies of the dangling OH stretch (νADH_d) for five structures of HW10A, HW10B, HW10C, HW10E, and HW10F are in good agreement with the experimental stretching frequency at 3716 cm^{-1} . The hydrogen bonded OH stretching frequencies (νADH_h) appear at ~ 3400 cm^{-1} , which is consistent with the experimental vibrational stretching frequencies. The ab initio calculations of the dangling OH stretching vibration in a tricoordinated water molecule of double acceptor–single donor (νAADH_d) for the above five structures are similar to the experimental frequency at 3689 cm^{-1} . The asymmetric ($\nu_a\text{ADDH}_h$) and symmetric ($\nu_s\text{ADDH}_h$) hydrogen bonded OH stretching frequencies in HW10A, HW10B, and HW10C are consistent with the experimental frequency. The vibrational stretching frequencies νAADH_h of HW10A, HW10B, HW10C, HW10E, and HW10F are 3436, 3442, 3433, 3428, and 3428 cm^{-1} , respectively, in good agreement with the experimentally observed vibrational frequencies of 3430 cm^{-1} . The calculated free-OH vibrational stretching frequencies in $\text{H}^+(\text{H}_2\text{O})_{10}$ appear in the region 3640–3742 cm^{-1} and the hydrogen bonded OH stretching frequencies appear in 3300–3625 cm^{-1} , consistent with the experiment spectra. Figure 2 shows the vibrational

spectra in the region of 3600–3800 cm^{-1} which are in good agreement with the experiment.

The strong symmetric $\nu_s(\text{H}_3\text{O}^+)$ and asymmetric $\nu_a(\text{H}_3\text{O}^+)$ stretching frequencies are predicted at 2858 and 2717 cm^{-1} for HW10A, and the strong $\nu_a(\text{H}_3\text{O}^+)$ frequency appears at 2733 cm^{-1} for HW10B, 2725 cm^{-1} for HW10C, and 2734 cm^{-1} for HW10F. These predicted frequencies are in reasonable agreement with the experimental frequencies at 2820 and 2730 cm^{-1} , respectively. The computed bending frequencies of hydronium (H_3O^+) are close to the experimental frequency at 1620 cm^{-1} .

Conclusion

At the complete basis set (CBS^D) limit for the CCSD(T) level of theory, the $\text{H}^+(\text{H}_2\text{O})_{10}$ cluster has three nearly isoenergetic 3D cage structures (two completely closed structures of HW10A and HW10B and one incompletely closed structure HW10C with one extra water molecule outside the closed cage) at 0 K. The three 3D cage structures are more stable in ZPE-corrected binding energy than other structures (by over ~ 1.0 kcal/mol, which indicates the reliability of our conclusion based on the CCSD(T)/CBS limit values). At ~ 150 K, the closed 3D structure for the protonated water clusters competes with the netlike structures. HW10C, which has two acceptor (A) type dangling water molecules, is the most stable, while there are two competing netlike structures (HW10E and HW10F). The HW10C structure is in good agreement with the Headrick et al.'s¹ experimental symmetric and asymmetric OH stretching peaks at 3650 and 3738 cm^{-1} for the free acceptor (A) type of dangling water molecules. At 250 K, two netlike structures (HW10F and HW10E) are the most stable, in agreement with the experiment of Miyazaki et al.²

Acknowledgment. This work was supported by KOSEF (WCU, R32-2008-000-10180-0; EPB Center, R11-2008-052-01000), BK21(KRF), GRL (KICOS), and KISTI (KSC-2008-K08-0002).

References and Notes

- (1) Headrick, J. M.; Diken, E. G.; Walters, R. S.; Hammer, N. I.; Christie, R. A.; Cui, J.; Myshakin, E. M.; Duncan, M. A.; Johnson, M. A.; Jordan, K. D. *Science* **2005**, *308*, 1765.
- (2) (a) Miyazaki, M.; Fujii, A.; Ebata, T.; Mikami, N. *Science* **2004**, *304*, 1134. (b) Shin, J. -W.; Hammer, N. I.; Diken, E. G.; Johnson, M. A.; Walters, R. S.; Jaeger, T. D.; Duncan, M. A.; Christie, R. A.; Jordan, K. D. *Science* **2004**, *304*, 1137.
- (3) (a) Asmis, K. R.; Pivonka, N. L.; Santambrogio, G.; Brummer, M.; Kaposta, C.; Neumark, D. M.; Wöste, L. *Science* **2003**, *299*, 1375. (b) Wu, C. C.; Lin, C. K.; Chang, H. C.; Jiang, J. C.; Kuo, J. L.; Klein, M. L. *J. Chem. Phys.* **2005**, *122*, 07431. (c) Jiang, J. C.; Wang, Y. S.; Chang, H. C.; Lin, S. H.; Lee, Y. T.; Niedner-Schatteburg, G.; Chang, H. C. *J. Am. Chem. Soc.* **2000**, *122*, 1398.
- (4) (a) Park, M.; Shin, I.; Singh, N. J.; Kim, K. S. *J. Phys. Chem. A* **2007**, *111*, 1069. (b) Lee, H. M.; Tarakeshwar, P.; Park, J. W.; Kolaski, M. R.; Yoon, Y. J.; Yi, H. -B.; Kim, W. Y.; Kim, K. S. *J. Phys. Chem. A* **2004**, *108*, 2949. (c) Christie, R. A.; Jordan, K. D. *J. Phys. Chem. A* **2002**, *106*, 8376.
- (5) Shin, I.; Park, M.; Min, S. K.; Lee, E. C.; Suh, S. B.; Kim, K. S. *J. Chem. Phys.* **2006**, *125*, 234305.
- (6) Karthikeyan, S.; Park, M.; Shin, I.; Kim, K. S. *J. Phys. Chem. A* **2008**, *112*, 10120.
- (7) Karthikeyan, S.; Kim, K. S. *Mol. Phys.* **2009**, *107*, 1169.
- (8) Singh, N. J.; Park, M.; Min, S. K.; Suh, S. B.; Kim, K. S. *Angew. Chem., Int. Ed.* **2006**, *45*, 3795.
- (9) Eigen, M.; Maeyer, L. D. *Proc. R. Soc. London, Ser. A* **1958**, *A* 247, 505.
- (10) Zundel, G.; Metzger, H. Z. *Phys. Chem. (Munich)* **1968**, *58*, 225.
- (11) (a) Ojamäe, L.; Shavitt, I.; Singer, S. J. *J. Chem. Phys.* **1998**, *109*, 5547. (b) Hodges, M. P.; Wales, D. J. *Chem. Phys. Lett.* **2000**, *324*, 279. (c) Iyengar, S. S.; Petersen, M. K.; Day, T. J. F.; Burnham, C. J.; Teige, V. E.; Voth, G. A. *J. Chem. Phys.* **2005**, *123*, 084309. (d) James, T.; Wales, D. J. *J. Chem. Phys.* **2005**, *122*, 134306. (e) Kuo, J. -L.; Klein, M. L. *J. Chem. Phys.* **2005**, *122*, 024516. (f) Wei, D.; Salahub, D. R. *J. Chem. Phys.* **1997**, *106*, 6086. (g) Valeev, E. F.; Schaefer, H. F., III. *J. Chem. Phys.* **1998**, *108*, 7197. (h) Iyengar, S. S. *J. Chem. Phys.* **2007**, *126*, 216101. (i) Petersen, M. K.; Iyengar, S. S.; Burnham, C. J.; Day, T. J. F.; Voth, G. A. *J. Phys. Chem.* **2004**, *108*, 14804. (j) McCoy, A. B.; Huang, X.; Carter, S.; Landeweer, M. Y.; Bowman, J. M. *J. Chem. Phys.* **2005**, *122*, 061101. (k) McCunn, L. R.; Roscioli, J. R.; Johnson, M. A.; McCoy, A. B. *J. Phys. Chem.* **2008**, *112*, 321.
- (12) (a) Pribble, R. N.; Zwier, T. S. *Science* **1994**, *265*, 75. (b) Gruenloh, C. J.; Carney, J. R.; Arrington, C. A.; Zwier, T. S.; Fredericks, S. Y.; Jordan, K. D. *Science* **1997**, *276*, 1678. (c) Buck, U.; Ettischer, I.; Melzer, M.; Buch, V.; Sadlej, J. J. *Phys. Rev. Lett.* **1998**, *80*, 2578. (d) Sadlej, J.; Buch, V.; Kazimirski, J. K.; Buck, U. *J. Phys. Chem.* **1999**, *103*, 4933. (e) Kim, K. S.; Tarakeshwar, P.; Lee, J. Y. *Chem. Rev.* **2000**, *100*, 4145. (f) Buck, U.; Huisken, F. *Chem. Rev.* **2000**, *100*, 3863. (g) Steinbach, C.; Andersson, P.; Melzer, M.; Kazimirski, J. K.; Buck, U.; Buch, V. *Phys. Chem. Chem. Phys.* **2004**, *6*, 3320.
- (13) (a) Kim, K. S.; Dupuis, M.; Lie, G. C.; Clementi, E. *Chem. Phys. Lett.* **1986**, *131*, 451. (b) Kim, J.; Kim, K. S. *J. Chem. Phys.* **1998**, *109*, 5886. (c) Ojamäe, L.; Shavitt, I.; Singer, S. J. *J. Chem. Phys.* **1998**, *109*, 5547. (d) Maheshwary, S.; Patel, N.; Sathyamurthy, N.; Kulkarni, A. D.; Gadre, S. R. *J. Phys. Chem. A* **2001**, *104*, 10525. (e) Fanourgakis, G. S.; Apra, E.; Xantheas, S. S. *J. Chem. Phys.* **2004**, *121*, 2655. (f) Lenz, A.; Ojamäe, L. *J. Phys. Chem.* **2006**, *110*, 13388.
- (14) (a) Hammer, N. I.; Shin, J. W.; Headrick, J. M.; Diken, E. G.; Roscioli, J. R.; Weddle, G. H.; Johnson, M. A. *Science* **2004**, *306*, 675. (b) Paik, D. H.; Lee, I. R.; Yang, D. S.; Baskin, J. S.; Zewail, A. H. *Science* **2004**, *306*, 672. (c) Verlet, J. R. R.; Bragg, A. E.; Kammrath, A.; Cheshnovsky, O.; Neumark, D. M. *Science* **2005**, *307*, 5706. (d) Hammer, N. I.; Roscioli, J. R.; Johnson, M. A. *J. Phys. Chem. A* **2005**, *109*, 7896.
- (15) (a) Lee, H. M.; Suh, S. B.; Tarakeshwar, P.; Kim, K. S. *J. Chem. Phys.* **2005**, *122*, 044309. (b) Lee, H. M.; Lee, S.; Kim, K. S. *J. Chem. Phys.* **2003**, *119*, 187. (c) Suh, S. B.; Lee, H. M.; Kim, J.; Lee, J. Y.; Kim, K. S. *J. Chem. Phys.* **2000**, *113*, 5273. (d) Jordan, K. D.; Wang, F. *Annu. Rev. Phys. Chem.* **2003**, *54*, 367.
- (16) (a) Nicely, A. L.; Miller, D. J.; Lisy, J. M. *J. Am. Chem. Soc.* in press. (b) Lisy, J. M. *Int. Rev. Phys. Chem.* **1997**, *16*, 267. (c) Vaden, T. D.; Forinash, B.; Lisy, J. M. *J. Chem. Phys.* **2002**, *117*, 4628. (d) Kim, J.; Lee, S.; Cho, S. J.; Mhin, B. J.; Kim, K. S. *J. Chem. Phys.* **1995**, *102*, 839. (e) Lee, H. M.; Kim, J.; Lee, S.; Mhin, B. J.; Kim, K. S. *J. Chem. Phys.* **1999**, *111*, 3995. (f) Kolaski, M.; Lee, H. M.; Choi, Y. C.; Kim, K. S.; Tarakeshwar, P.; Miller, D. J.; Lisy, J. M. *J. Chem. Phys.* **2007**, *126*, 074302. (g) Lee, H. M.; Tarakeshwar, P.; Park, J. W.; Kolaski, M. R.; Yoon, Y. J.; Yi, H. -B.; Kim, W. Y.; Kim, K. S. *J. Phys. Chem. A* **2004**, *108*, 2949. (h) Karthikeyan, S.; Singh, J. N.; Park, M.; Kumar, R.; Kim, K. S. *J. Chem. Phys.* **2008**, *128*, 244304. (i) Karthikeyan, S.; Singh, J. N.; Kim, K. S. *J. Phys. Chem. A* **2008**, *112*, 6527.
- (17) (a) Lee, H. M.; Suh, S. B.; Lee, J. Y.; Tarakeshwar, P.; Kim, K. S. *J. Chem. Phys.* **2000**, *112*, 9759. (b) Lee, H. M.; Suh, S. B.; Kim, K. S. *J. Chem. Phys.* **2001**, *114*, 10749.
- (18) (a) Li, Z.; Scheraga, H. A. *Proc. Natl. Acad. Sci. U.S.A.* **1987**, *84*, 6611. (b) Day, P. N.; Pachter, R.; Gordon, M. S.; Merrill, G. N. *J. Chem. Phys.* **2000**, *12*, 2063.
- (19) Elstner, M.; Porezag, D.; Jungnickel, G.; Elsner, J.; Haugk, M.; Frauenheim, T.; Suhai, S.; Seifert, G. *Phys. Rev. B* **1998**, *58*, 7260.
- (20) (a) Becke, A. D. *J. Chem. Phys.* **1993**, *98*, 5648. (b) Lee, C.; Yang, W.; Parr, R. G. *Phys. Rev. B* **1988**, *37*, 785.
- (21) Frisch, M. J.; Trucks, G. W.; Schlegel, H. B.; Scuseria, G. E.; Robb, M. A.; Cheeseman, J. R.; Montgomery, J. A., Jr.; Vreven, T.; Kudin, K. N.; Burant, J. C.; Millam, J. M.; Iyengar, S. S.; Tomasi, J.; Barone, V.; Mennucci, B.; Cossi, M.; Scalmani, G.; Rega, N.; Petersson, G. A.; Nakatsuji, H.; Hada, M.; Ehara, M.; Toyota, K.; Fukuda, R.; Hasegawa, J.; Ishida, M.; Nakajima, T.; Honda, Y.; Kitao, O.; Nakai, H.; Klene, M.; Li, X.; Knox, J. E.; Hratchian, H. P.; Cross, J. B.; Bakken, V.; Adamo, C.; Jaramillo, J.; Gomperts, R.; Stratmann, R. E.; Yazyev, O.; Austin, A. J.; Cammi, R.; Pomelli, C.; Ochterski, J. W.; Ayala, P. Y.; Morokuma, K.; Voth, G. A.; Salvador, P.; Dannenberg, J. J.; Zakrzewski, V. G.; Dapprich, S.; Daniels, A. D.; Strain, M. C.; Farkas, O.; Malick, D. K.; Rabuck, A. D.; Raghavachari, K.; Foresman, J. B.; Ortiz, J. V.; Cui, Q.; Baboul, A. G.; Clifford, S.; Cioslowski, J.; Stefanov, B. B.; Liu, G.; Liashenko, A.; Piskorz, P.; Komaromi, I.; Martin, R. L.; Fox, D. J.; Keith, T.; Al-Laham, M. A.; Peng, C. Y.; Nanayakkara, A.; Challacombe, M.; Gill, P. M. W.; Johnson, B.; Chen, W.; Wong, M. W.; Gonzalez, C.; and Pople, J. A. *Gaussian 03, Revision C.02*; Gaussian, Inc.: Wallingford, CT, 2004.
- (22) Werner, H. -J.; Knowles, P. J.; Lindh, R.; Manby, F. R.; Schutz, M.; Celani, P.; Korona, T.; Rauhut, G.; Amos, R. D.; Bernhardsson, A.; Berning, A.; Cooper, D. L.; Deegan, M. J. O.; Dobbyn, A. J.; Eckert, F.; Hampel, C.; Hetzer, G.; Lloyd, A. W.; McNicholas, S. J.; Meyer, W.; Mura, M. E.; Nicklass, A.; Palmieri, P.; Pitzer, R.; Schumann, U.; Stoll, H.; Stone, A. J.; Tarroni, R.; Thorsteinsson, T. MOLPRO, version 2006.1, a package of ab initio programs, see <http://www.molpro.net>.
- (23) Lee, S. J.; Chung, H. Y.; Kim, K. S. *Bull. Korean Chem. Soc.* **2004**, *25*, 1061.
- (24) (a) Helgaker, T.; Ruden, T. A.; Jorgensen, P.; Olsen, J.; Klopper, W. *J. Phys. Org. Chem.* **2004**, *17*, 913. (b) Helgaker, T.; Klopper, W.; Koch, H.; Noga, J. *J. Chem. Phys.* **1997**, *106*, 9639-9646.
- (25) (a) Min, S. K.; Lee, E. C.; Lee, H. M.; Kim, D. Y.; Kim, D.; Kim, K. S. *J. Comput. Chem.* **2008**, *29*, 1208. (b) Lee, E. C.; Kim, D.; Jurečka, P.; Tarakeshwar, P.; Hobza, P.; Kim, K. S. *J. Phys. Chem. A* **2007**, *111*, 3446.
- (26) (a) Császár, A. G.; Allen, W. D.; Schaefer III, H. F. *J. Chem. Phys.* **1998**, *108*, 9751. (b) Sinnokrot, M. O.; Sherrill, C. D. *J. Phys. Chem. A* **2004**, *108*, 10200.
- (27) (a) Benedict, W. S.; Gailar, G.; Plyler, E. K. *J. Chem. Phys.* **1956**, *24*, 1139. (b) Fraley, P. E.; Rao, K. N. *J. Mol. Spectrosc.* **1969**, *29*, 348.
- (28) (a) Kim, K. S.; Mhin, B. J.; Choi, U.-S.; Lee, K. *J. Chem. Phys.* **1992**, *97*, 6649. (b) Kim, J.; Lee, J. Y.; Lee, S.; Mhin, B. J.; Kim, K. S. *J. Chem. Phys.* **1995**, *102*, 310.
- (29) Pak, C.; Lee, H. M.; Kim, J. C.; Kim, D.; Kim, K. S. *Struct. Chem.* **2005**, *16*, 187.